

Degradation of Tributyltin Chloride in Water Photoinduced by Iron(III)

Gilles Mailhot,¹ Michel Astruc² and Michèle Bolte^{1*}

¹Laboratoire de Photochimie Moléculaire et Macromoléculaire, Université Blaise Pascal, UMR CNRS 6505, F-63177 Aubière Cedex, France

²Laboratoire de Chimie Analytique, EP CNRS 132 CBIE, Université de Pau et des Pays de l'Adour, F-64000 Pau, France

The degradation of tributyltin chloride (TBT) photoinduced by iron(III) was investigated. Upon irradiation at $\lambda_{\text{excitation}} > 300$ nm a photo-redox process was observed, yielding iron(II) and $\cdot\text{OH}$ radicals. The disappearance of TBT was proved to involve only an attack by $\cdot\text{OH}$ radicals: the quantum yield of TBT disappearance was determined. A wavelength effect was observed; the shorter the excitation wavelength, the higher the rate of TBT disappearance. Most of the photoproducts were identified and the mechanism of degradation was elucidated. The main route to degradation is a stepwise debutylation of TBT to di- and mono-butyltin with final formation of inorganic tin. The complete mineralization of TBT was achieved with long irradiation times, leading to innocuous inorganic tin. Copyright © 1999 John Wiley & Sons, Ltd.

Keywords: tributyltin; photodegradation; iron(III); aqueous solution; $\cdot\text{OH}$ radicals; dibutyltin; monobutyltin

Received 23 December 1997; accepted 30 April 1998

INTRODUCTION

Organotin compounds have been produced since the late 1930s and world consumption in 1989 was estimated to be 35×10^6 tons.¹ Among these compounds, tributyltin (TBT) has been used extensively: it is employed in antifouling paints on ships, boats and docks, although its use, in this domain, has been prohibited or restricted in several countries.² However, TBT also acts as a fungicide, bactericide, insecticide and preservative for wood,

* Correspondence to: Michèle Bolte, Laboratoire de Photochimie Moléculaire et Macromoléculaire, Université Blaise Pascal, UMR CNRS 6505, F-63177 Aubière Cedex, France.
E-mail: boltem@cicsun.univ-bpclermont.fr

textiles, paper, leather and electrical equipment. Butyltin compounds such as dibutyltin (DBT) and monobutyltin (MBT) are also used as stabilizers for PVC and other plastics.

Although inorganic tin compounds are basically harmless, some organotin compounds are very toxic to both animal and vegetable life. Thus very low levels of TBT are lethal or cause reduced growth and reproduction of commercial shellfish.³ These effects are particularly important for juvenile life forms of other organisms.^{4,5} TBT is among the most toxic compounds to aquatic ecosystems known so far.⁶

Environmental fates of these organotin compounds in sludge,⁷ sediments,⁸ micro-organisms and aquatic and marine environments have been studied extensively.^{9–12} In summary, the abiotic process is generally considered as being less important than biotic action, although physico-chemical degradation occurs. Despite abiotic and biotic degradation, tributyltin has been shown to exist at toxic levels in the aquatic environment.

Among the different abiotic degradation processes, solar irradiation is one of the main factors responsible for TBT degradation in the environment. Energetically, only the ultraviolet (UV) wavelengths (295–320 nm) are likely to cause direct photolysis of tributyltin. Numerous investigations have confirmed photolytic degradation of butyltin compounds.^{13–16} All these authors indicated that degradation occurs by a stepwise debutylation mechanism to less toxic compounds. However, this process has its limitations as the maximum absorption wavelength of butyltin compounds is within the region 190–250 nm. Consequently, TBT species are degraded very slowly by natural sunlight (half-life >89 days).¹³ Moreover, Duhamel *et al.*¹⁵ indicated that, after three months under irradiation by sunlight, the degradation of TBT reached a stable value (roughly 50% of degradation). Because of the very slow degradation, Navio *et al.*¹⁷ studied the degradation of butyltin

compounds by the photocatalytic action of TiO_2 under UV illumination in aqueous solution. However, they concluded that butyltins offer high resistance to photodegradation by either photolytic or TiO_2 -photoassisted processes. The apparent observed quantum yields of TiO_2 -photoassisted processes were about 10^{-7} , and lower than that observed for the photolytic process.

Degradation of several water pollutants photo-induced by iron(III) were studied in our laboratory.^{18–21} In all cases, we concluded that the degradation photoinduced by iron(III) was an interesting process for the elimination of pollutants in aqueous solution.

In the work reported here, we investigated the degradation of butyltin compounds photoinduced by iron(III) in aqueous solution under different experimental conditions. We studied the photo-degradation process of TBT with a kinetic and analytical approach. Most of the photoproducts were identified and a mechanism of degradation has been proposed.

MATERIALS AND METHODS

Reagents and solutions

Tributyltin chloride (TBT; 96%), dibutyltin dichloride (DBT; 96%), monobutyltin trichloride (MBT; 96%) and tin(IV) chloride pentahydrate (>98%) were purchased from Aldrich. Tin(II) chloride dihydrate (98%) was a Prolabo product. Organotin concentration is given as parts per million (ppm) of tin. The range investigated in this work was 0–2 ppm, which corresponds to $0\text{--}1.7 \times 10^{-5} \text{ mol l}^{-1}$ as organotin derivative. These solutions were obtained by diluting stock solutions of organotins prepared in acetonitrile (Carlo Erba reagent, HPLC grade) at 1000 mg tin per litre (1000 ppm). Methanol, scavenger of $\cdot\text{OH}$ radicals, is prohibited in this work.

Ferric perchlorate nonahydrate [$\text{Fe}(\text{ClO}_4)_3 \cdot 9\text{H}_2\text{O}$ >97%] and barium hydroxide octahydrate ($\geq 98\%$) were Fluka products; they were kept in a desiccator. The iron(III) solutions for these studies were prepared by diluting stock solutions ($2.0 \times 10^{-3} \text{ mol l}^{-1}$ as $\text{Fe}(\text{ClO}_4)_3 \cdot 9\text{H}_2\text{O}$) to the appropriate iron(III) concentration. Sodium tetraethylborate (NaBEt_4 ; $\leq 98\%$) was a Strem Chemical product; it was kept at 6°C and under argon. The solutions were prepared by dissolving 20 mg NaBEt_4 in 1 cm^3 of deionized water. 8-Hydroxyquinoline-5-

sulphonic acid monohydrate (HQSA; 98%) and 5,5-dimethyl-1-pyrroline *N*-oxide (DMPO; 97%) were purchased from Aldrich. Iso-octane and isopropanol were Merck products (HPLC grade).

All solutions were prepared with deionized ultrapure water ($\rho = 18.2 \text{ M}\Omega \text{ cm}$). When necessary, the solutions were degassed by bubbling with argon for 45 min at room temperature. The pH was measured with an Orion pH meter to ± 0.02 pH unit [pH = 3.0 for a solution with a concentration in iron(III) equal to $3 \times 10^{-4} \text{ M}$]. The ionic strength was not controlled.

Apparatus

In order to measure quantum yields, monochromatic irradiation at 296, 313 and 365 nm was carried out with a high-pressure mercury lamp (Osram HBO 200 W) equipped with a grating monochromator (Bausch and Lomb). The beam was parallel and the reactor was a cylindrical quartz cell of 1 cm path length. The light intensity was measured by ferrioxalate actinometry:²² $I_{0,365 \text{ nm}} \approx 4.0 \times 10^{15}$, $I_{0,313 \text{ nm}} \approx 2.0 \times 10^{15}$ and $I_{0,296 \text{ nm}} \approx 9.8 \times 10^{14} \text{ photons s}^{-1} \text{ cm}^{-2}$.

The apparatus for irradiation at $\lambda_{\text{exc.}} = 365 \text{ nm}$ was an elliptical stainless steel cylinder. A high-pressure mercury lamp (Philips HPW type 125 W), where emission at 365 nm was selected by an inner filter, was located at a focal axis of the elliptical cylinder. The reactor, a water-jacketed Pyrex tube (diameter 2.8 cm), was centred at the other focal axis. The reaction medium was well stirred. The unit delivered an intensity $I_a \approx 3.45 \times 10^{15} \text{ photons s}^{-1} \text{ cm}^{-3}$, over a large volume (60 ml).

Solar irradiation was carried out in a Pyrex cylindrical reactor during summertime in Clermont-Ferrand (latitude 46°N , 400 m above sea level).

UV-visible spectra were recorded on a Cary 3 double-beam spectrophotometer. ESR spectra were obtained using a Bruker ER-200D spectrometer at 9.30 GHz with a modulation field of 100 KHz. A xenon mercury Hanovia lamp was used for irradiation in the ESR spectrometer cavity ($\lambda \geq 305 \text{ nm}$).

Gas-chromatographic analysis was performed using a Delsi GC DI 700 equipped with a flame ionization detector (GC-FID). A DB-1 capillary column (dimethylpolysiloxane phase, J&W Scientific, Folson, CA, USA), dimensions $30 \text{ m} \times 0.25 \text{ mm}$ i.d. with a film thickness of $0.25 \mu\text{m}$, was used. Nitrogen carrier gas was used with a flow rate of 1 ml min^{-1} . Samples ($2 \mu\text{l}$) were introduced onto the column in the splitless injection mode with

a splitless time of 1 min. The injector temperature was 290 °C and the FID temperature was 280 °C.

Gas chromatography–mass spectrometry (GC–MS) analysis was performed using a Hewlett–Packard model 5985 gas chromatograph/mass spectrometer system. An Optima 5 (Macherey–Nagel) capillary column, dimensions 25 m × 0.25 mm i.d. with a film thickness of 0.25 μm, was used. The injector temperature was 250 °C and the sample was injected in the splitless injection mode for 1 min. Standard EI (70 eV) conditions were used with a source temperature of 250 °C, the mass range being from 20 to 500 m/z units. Helium was used as a carrier gas.

In all gas-chromatography analysis, the GC oven temperature was maintained at 70 °C for 1 min and increased at 20 °C min^{-1} to a maximum of 270 °C where it was held for 5 min.

Analysis

Organotin compounds were analysed after ethylation/extraction in the conditions described by Carlier–Pinasseau *et al.*²³ Sodium tetraethylborate was used as an alkylation reagent. Ethylation and extraction of organotin compounds could be performed in water in a one-step procedure. A $165 \pm 10 \text{ cm}^3$ Pyrex flask with a narrow neck was used for this operation: 50 cm^3 of water and 200 μl of sodium tetraethylborate at 2% were introduced and the pH was then adjusted to 4.5 using an appropriate quantity of sodium acetate and acetic acid buffer. Isooctane (0.5 cm^3) was added and vigorous swirling was obtained by magnetic stirring (1250 rpm for 40 min). The swirling was stopped and the organic phase was transferred into a vial for injection into the gas chromatograph. In these conditions, it was possible to identify inorganic tin by GC–MS analysis but not to quantify it.

Repeated injections (four) were carried out to investigate the reproducibility of the peak area in GC–FID. External calibration was performed for MBT, DBT and TBT in water using concentrations of 0–2 ppm Sn (Fig. 1). Regression coefficients (respectively 0.9969, 0.9975 and 0.9999) demonstrated a good linearity of calibration in the concentration domain. These calibration curves were also used to estimate roughly the concentration of the oxidized derivatives of TBT, DBT and MBT.

The method of measuring the monomeric concentration of iron(III) was modified from Kuenzi's procedure.²⁴ 8-Hydroxyquinoline-5-sulphonic acid (HQSA, 1 cm^3 , 0.05 M) and acetic acid buffer (pH

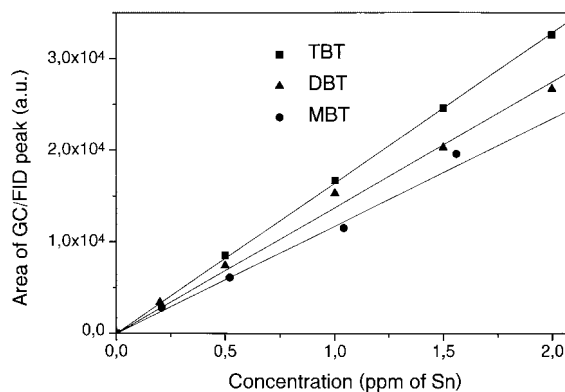


Figure 1 Calibration curves of tin derivatives by GC–FID after derivatization: ■, TBT; ▲, DBT; ●, MBT.

4.6) were poured in a 10 cm^3 volumetric flask, to which 8 cm^3 of sample were added and rapidly mixed. Within 30 s of mixing, the absorbance of the tris (8-hydroxyquinoline-5-sulfonate) (HQS) complex with iron(III), $\text{Fe}(\text{HQS})_3$, was measured at = 572 nm. The same mixture with 8 cm^3 of water was used as a blank. HQSA reacted much more rapidly with monomeric iron(III) species than with either iron(III) dimer or iron(III) oligomers. The complex $\text{Fe}(\text{HQS})_3$ absorbed in a spectral region (572 nm) where neither the iron(III) dimer nor iron(III) polymer/precipitate absorb. Two ϵ_{572} values for $\text{Fe}(\text{HQS})_3$ have been reported: $\epsilon_{572} = 5180 \text{ l mol}^{-1} \text{ cm}^{-1}$ by Kuenzi,²⁴ and $\epsilon_{572} = 4970 \text{ l mol}^{-1} \text{ cm}^{-1}$ by Faust and Hoigné.²⁵ An averaged value of $5075 \text{ l mol}^{-1} \text{ cm}^{-1}$ was used in this work.

Iron(II) concentration was determined by complexometry with *o*-phenanthroline, using $\epsilon_{510} = 1.118 \times 10^4 \text{ l mol}^{-1} \text{ cm}^{-1}$ for the iron(II)–phenanthroline complex.²²

The carbon dioxide (CO_2) produced was determined as BaCO_3 . It was swept out of the reactor by a flow of oxygen (relieved from CO_2 traces by bubbling into concentrated $\text{Ba}(\text{OH})_2$ solution) and trapped in two consecutive 0.012 mol l^{-1} $\text{Ba}(\text{OH})_2$ solutions. The solutions were collected, BaCO_3 was allowed to precipitate and the excess of $\text{Ba}(\text{OH})_2$ was titrated with a 0.010 mol l^{-1} HCl solution. A blank experiment was performed under the same conditions but without TBT.

RESULTS

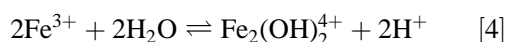
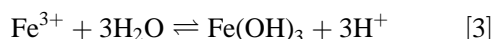
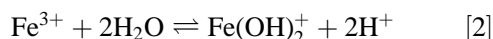
All organotin concentrations are expressed as tin

(mg l⁻¹ or ppm). The initial concentration of iron(III) in the solution was generally 3 × 10⁻⁴ mol l⁻¹.

Characterization of iron(III) and TBT in aqueous solution

Tributyltin chloride (TBT) is only slightly soluble in water, with a maximum solubility of approx. 10 ppm. The TBT concentration of the initial solutions used in this work was 2 ppm. At pH = 5.9 ± 0.1, the natural pH of a 2 ppm TBT solution, there was no degradation of TBT when the solution was kept in the dark at room temperature. TBT is stable in aqueous solution. The UV-visible spectrum of TBT presents a very weak absorption between 280 (ε = 2.72 l mol⁻¹ cm⁻¹) and 360 nm (ε = 0.06 l mol⁻¹ cm⁻¹).¹³

The hydrolysis of iron(III) in dilute aqueous solution is a complex phenomenon that can be described by the equilibria represented by Eqns [1]–[4].²⁵ For simplicity, coordinated water molecules are not included in the chemical formulae; for example, Fe(OH)²⁺ refers to Fe(OH)(H₂O)₅²⁺.



In order to interpret accurately the absorption spectrum and photochemical behaviour, it is essential to know the hydrolytic speciation of iron(III). Under our experimental conditions ([Fe(III)] = 3 × 10⁻⁴ mol l⁻¹ and pH = 3.10 ± 0.10), Fe(OH)²⁺ is the predominant monomeric iron(III) hydroxy complex.²⁵ However, the concentration of monomeric species rapidly decreased after the dissolution of ferric perchlorate in water. This disappearance was attributed to the possible formation of soluble oligomeric species or aggregates followed by the precipitation of amorphous Fe(OH)₃.²⁶ Under our experimental conditions, this precipitation has never been observed. It appeared that the percentage of Fe(OH)²⁺, i.e. ([Fe(OH)²⁺]/[total iron(III)]) × 100, the most photoreactive species,²⁵ strongly depended on the age of the ferric solution (before and after dilution) and on the starting concentration. By the HQSA method (see Analysis section) we were able to measure the concentration of Fe(OH)²⁺ in solution. Fe(OH)²⁺ generally comprised 40% of our starting solutions.

The TBT–iron(III) mixture in aqueous solution

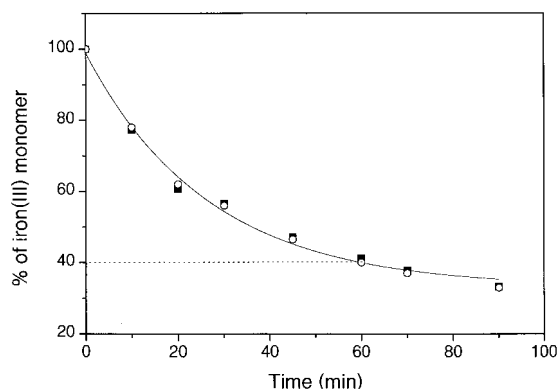
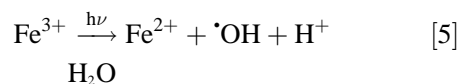


Figure 2 Percentage of iron(III) monomeric species in aqueous solution: ■, with TBT (2 ppm); ○, without TBT.

was thermally stable for a few weeks (in the dark at room temperature) in terms of TBT concentration. The resulting UV-visible spectrum was the sum of the UV spectra of TBT and iron(III): there was no evidence of complexation in the ground state. Under our experimental conditions, the decrease of Fe(OH)²⁺ concentration was not affected by the presence of TBT (Fig. 2). TBT does not interfere in the evolution of iron(III) species. This result is in agreement with the fact that no complexation between iron(III) and TBT was found.

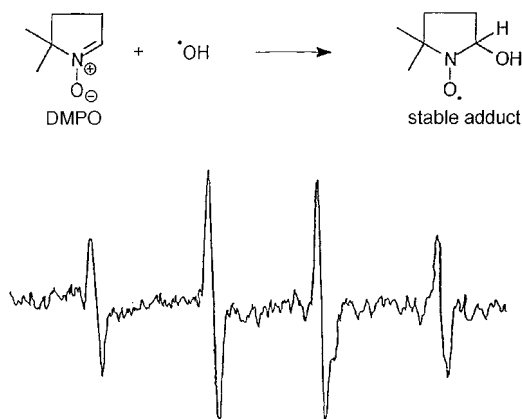
Photochemical behaviour

Iron(III) aquo complexes are known to undergo a photochemical process through an internal electron transfer giving rise to [•]OH radicals and iron(II) (Eqn [5])²⁸



The quantum yields of iron(II) and of [•]OH radicals were measured by different authors as a function of the irradiation wavelength.^{25,27,28} The increase in quantum yield always observed when the excitation wavelength decreased is attributed to the kinetic energy required for the ejection of [•]OH radicals from the solvent cage.²⁷

Upon irradiation at 365 nm, the light was only absorbed by iron(III) species; TBT does not absorb significantly at λ > 290 nm. The formation of [•]OH radicals, upon irradiation (λ ≥ 305 nm) was confirmed by ESR spectroscopy. For spin-trapping



1:2:2:1 quartet pattern ($a = 14.6$ G) was observed due to the equality of a_{N} and a_{H} .

Figure 3 Spin-trapping experiments with DMPO (1 mg cm^{-3} in solution) by ESR spectroscopy upon irradiation ($\lambda \geq 305$ nm): $[\text{Fe(III)}]_0 = 3 \times 10^{-4} \text{ mol l}^{-1}$; $[\text{TBT}]_0 = 2$ ppm.

experiments, 5,5-dimethyl-1-pyrroline-1-oxide (DMPO) (1 mg cm^{-3}), was added to the iron(III) and TBT solution. Upon irradiation, a 1:2:2:1 quartet ($a = 14.6$ G) was observed, characteristic of the stable adduct with $\cdot\text{OH}$ radicals (Fig. 3). The existence of a quartet instead of a triplet of doublet was due to the identical value of the coupling constants a_{N} and a_{H} . In the presence of 1% of isopropanol (used as a scavenger of $\cdot\text{OH}$ radicals) no signal was detected in ESR spectroscopy and the

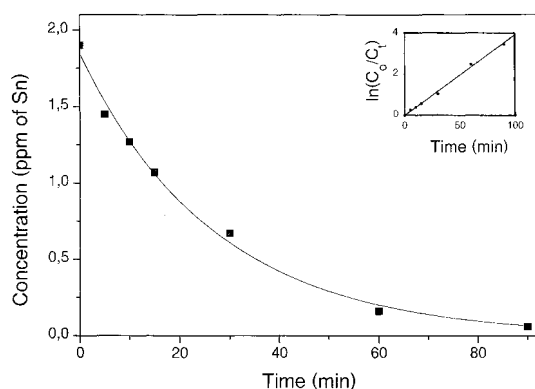


Figure 4 Decrease in TBT concentration upon irradiation at 365 nm: $[\text{Fe(III)}]_0 = 3 \times 10^{-4} \text{ mol l}^{-1}$ (with 40% monomeric species); $[\text{TBT}]_0 = 2$ ppm. The insert shows the first-order disappearance of TBT (correlation coefficient > 0.99).

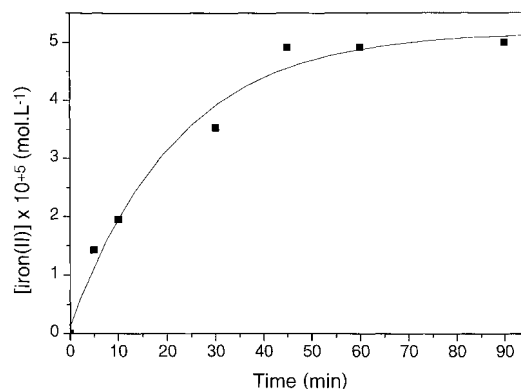


Figure 5 Formation of iron(II) as a function of irradiation time at 365 nm: $[\text{Fe(III)}]_0 = 3 \times 10^{-4} \text{ mol l}^{-1}$ (with 40% monomeric species); $[\text{TBT}]_0 = 2$ ppm.

degradation of TBT was totally inhibited (cf. later). These two results show that TBT degradation is only due to the $\cdot\text{OH}$ radicals produced upon irradiation of iron(III) aqueous solution.

Upon irradiation at $\lambda = 365$ nm of a TBT-iron(III) mixture with 40% of monomeric species Fe(OH)^{2+} , the concentration of TBT decreased continuously (Fig. 4). The disappearance of TBT appeared to follow first-order kinetics, a good linear relationship being obtained when plotting $\ln([\text{TBT}]_0/[\text{TBT}]) = f$ (irradiation time), $k_{\text{obs.}} = 0.039 \text{ min}^{-1}$. Simultaneously, we observed the formation of iron(II), monitored by complexometry with *o*-phenanthroline (Fig. 5). The concentration of iron(II) increased quickly, then reached a plateau for longer irradiation times. This plateau can be assigned to the establishment of a steady state with the re-oxidation of iron(II) species. The quantum yield of iron(II) formation and of TBT disappearance (ϕ_{TBT}) was evaluated as 7.5×10^{-3} and 1.6×10^{-3} respectively.

We measured the quantum yields of TBT disappearance by GC-FID at different wavelengths. The results are summarized in Table 1.

The quantum yields of TBT disappearance are strongly dependent on wavelength. This result has

Table 1 Quantum yield of TBT disappearance as a function of irradiation wavelength

λ (nm)	365	334	313	296
ϕ_{TBT}	1.6×10^{-3}	7.0×10^{-3}	1.0×10^{-2}	1.85×10^{-2}

to be related to the increasing efficiency of $\cdot\text{OH}$ radical formation when the wavelength decreases. We checked that direct photolysis of TBT was negligible at all these wavelengths.

The lifetime of TBT when it undergoes the attack by $\cdot\text{OH}$ radicals arising from the excitation of aqueous iron(III) solution was estimated as described by ECETOC.²⁹ It is based on the experimentally determined quantum yield of TBT disappearance, the absorption spectrum of iron(III) and the solar irradiation intensities,³⁰ and the half-lifetime $\tau_{1/2}$ is defined by Eqn [6]:

$$\tau_{1/2} = \frac{\ln 2}{2300 \int_{\lambda_1}^{\lambda_2} \phi(\lambda) \cdot I_0(\lambda) \cdot \varepsilon(\lambda) \cdot d\lambda} \quad [6]$$

where $\tau_{1/2}$ = half-lifetime (s);

ϕ = quantum yield of TBT degradation (molecules per photon) at wavelength λ in the range λ_1 – λ_2 ;

I_0 = intensity of sunlight at wavelength λ (Einstein $\text{cm}^{-2} \text{s}^{-1} \text{nm}^{-1}$);

ε = molar extinction coefficient of iron(III) species at wavelength λ ($1 \text{ mol}^{-1} \text{cm}^{-1}$); 2300 = factor taking into account the conversion of litres into cm^3 and of decadic units into Napierian logarithms.

The half-lifetimes were estimated to be in the range 2–3 h in June and 15–16 h in January under local conditions. Even though the formula was established for compounds undergoing a direct photolysis, it provides satisfactory results (see below).

Analysis of Photoproducts

For the analysis and identification of the photoproducts we irradiated three types of solution (Fe + TBT, Fe + DBT and Fe + MBT) with a $3 \times 10^{-4} \text{ mol l}^{-1}$ iron(III) and a 2 ppm (i.e. $1.68 \times 10^{-5} \text{ mol l}^{-1}$) organotin concentration. The analysis by GC-FID, after derivatization with NaBEt_4 , showed that several photoproducts were formed during the degradation of TBT photoinduced by iron(III). The concentrations of TBT, DBT and MBT were determined from calibration curves obtained with authentic samples. DBT and MBT were the major photoproducts in the early stages of the reaction.

The TBT, DBT and MBT concentrations, as a function of irradiation time, are reported in Fig. 6. DBT and MBT concentrations go through a maximum, and completely disappear for longer

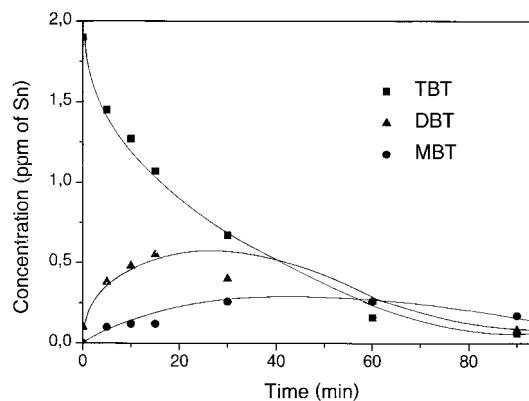


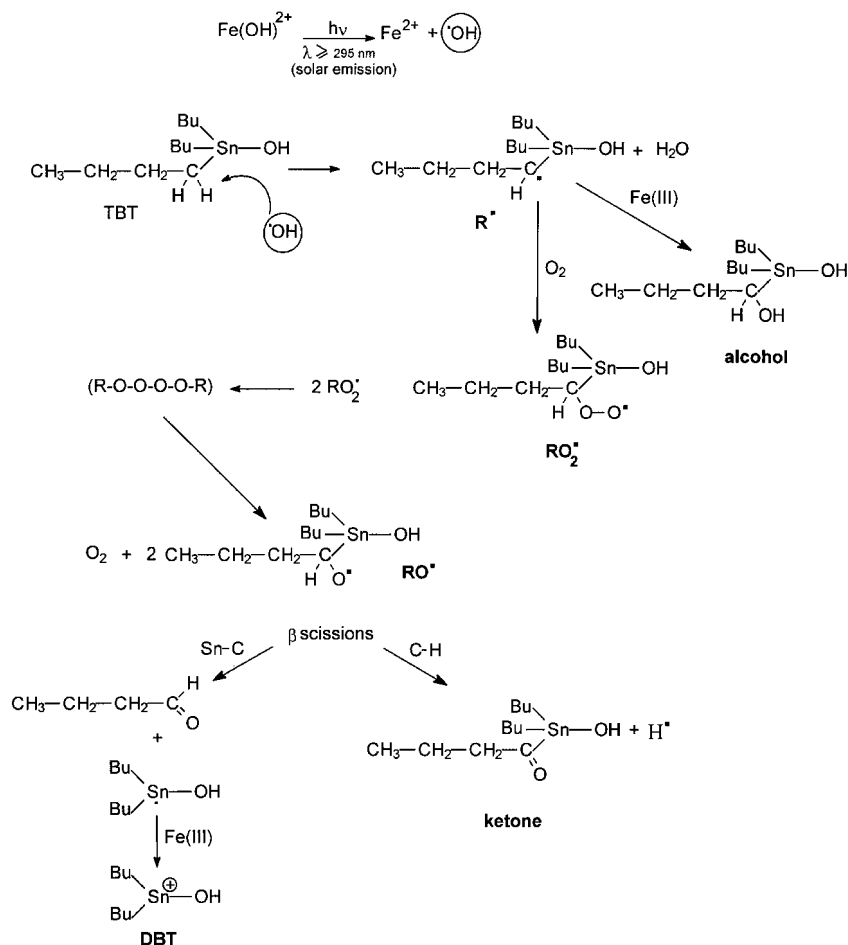
Figure 6 Evolution of TBT, DBT and MBT concentrations as a function of irradiation time at 365 nm: $[\text{Fe(III)}]_0 = 3 \times 10^{-4} \text{ mol l}^{-1}$ (with 40% monomeric species); $[\text{TBT}]_0 = 2 \text{ ppm}$; ■, TBT; ▲, DBT; ●, MBT.

irradiations. A continuously increasing deficit in the mass balance appears with irradiation time (Table 2) when only these products are considered.

Other photoproducts were identified by GC-MS analysis. Inorganic tin, identified as SnEt_4 , was present in the irradiated solution. Several oxidized organotin derivatives, ketones and alcohols, were also identified at much lower concentrations. In the early stages of the reaction, the ratio between the formation of DBT and of TBT ketones remained roughly constant and equal to 8:1. The formation of DBT was strongly favoured relative to the oxidation of the butyl chain (cf. scissions in the mechanism). Two ketones ($M + 14$) and two alcohols ($M + 16$) were the results of the degradation of TBT. Under these conditions the formation of alcohols was a minor route of TBT transformation. It is worth noting that all the photoproducts appeared as a family corresponding to the attack on TBT, DBT and MBT by a similar process: we also observed the formation of two ketones and two

Table 2 TBT, DBT and MBT concentrations and mass balance in terms of butyltin compounds as a function of irradiation time

	Irradiation time (min)						
	0	5	10	15	30	60	90
TBT (ppm)	1.90	1.45	1.27	1.07	0.67	0.16	0.06
DBT (ppm)	0.10	0.38	0.48	0.55	0.40	0.26	0.08
MBT (ppm)	0	0.10	0.12	0.12	0.26	0.26	0.17
Mass balance (ppm)	2.00	1.93	1.87	1.74	1.33	0.68	0.21



Scheme 1 Proposed mechanism for iron(III)-photoinduced degradation of TBT.

alcohols during the oxidation of DBT and MBT. A minor family, the parent peak of which corresponded to the mass of the starting organotin derivative, was not identified.

For irradiation times of 24 h, the degradation of TBT and all the photoproducts were almost completely achieved. At the end of irradiation, we only detected the presence of inorganic tin in the solution.

For long irradiation times (>40 h) we obtained a 97% yield of CO_2 , considering that total oxidation of TBT should lead to 12 mol CO_2 per mol TBT.

Effect of oxygen

Oxygen exerted no significant influence on the quantum yield of TBT disappearance: the rate of degradation of TBT decreased very slightly in the

absence of oxygen. In contrast, the absence of oxygen affected the formation of the photoproducts very strongly: the rate of ketone formation was divided by seven whereas that of alcohols was multiplied by a factor of five.

Irradiation under solar light and projection to environment

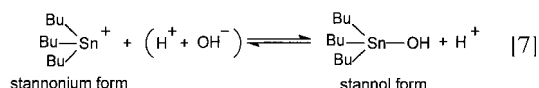
A mixture of TBT (2 ppm) and iron(III) [$3 \times 10^{-4} \text{ mol l}^{-1}$, with 40% monomeric $\text{Fe}(\text{OH})^{2+}$] was exposed to solar light during a sunny day in July 1996. After 2 h, about 50% of the TBT had disappeared and the photoproducts were analogous in nature to those observed upon excitation at 365 nm. This value is in good agreement with the estimate of the half-lifetime obtained from the ECETOC formula.²⁹ However, under solar irradiation

tion and for the same percentage conversion of TBT, the concentrations of the photoproducts detected in the solution decreased by 90%. After 8 h of irradiation, no more organotin was detectable by GC-FID. The degradation of TBT and the other organotins was complete.

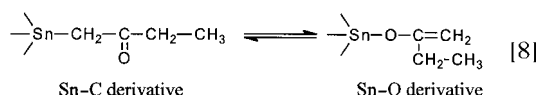
MECHANISM AND DISCUSSION

Iron(III) species are the only absorbing species when a mixture of TBT and iron(III) in aqueous solution is irradiated at 365 nm. Iron(III) aqueous species are known to undergo a redox reaction giving rise to iron(II) and $\cdot\text{OH}$ radicals, according to Eqn [5]. Among the iron(III) species present in the solution, $\text{Fe}(\text{OH})^{2+}$, the monomeric form present under our experimental conditions, is the most photoreactive one.²⁵ In terms of TBT degradation, the mechanism only involves attack by $\cdot\text{OH}$ radicals, as evidenced by the total inhibition observed when 1% isopropanol is added to the solution. The rate of TBT degradation is strongly affected by the excitation wavelength: it increases when excitation is reduced from 365 to 296 nm.

The nature of the photoproducts, particularly the major ones (DBT, MBT, Sn), shows that attack of $\cdot\text{OH}$ radicals occurs mainly by abstraction of a hydrogen atom from the carbon of a butyl group in the α -position to tin. However, the attack of the electrophilic $\cdot\text{OH}$ radicals is disfavoured by the positive charge on the stannonium form, so the attack on the carbon in the α -position may be explained by partial hydrolysis leading to the more favorable stannol form (Eqn [7]):



The presence of two different alcohols and ketones shows that attack of $\cdot\text{OH}$ radicals can also take place on the carbon in the β -position to tin. In addition, the attack of $\cdot\text{OH}$ radicals on the carbon in the β -position generates the corresponding ketone, known to be in equilibrium with an 'Sn-O' derivative (Eqn [8]).^{31,32}



Sn-O derivatives of TBT, DBT and MBT were

detected by GC-MS with the presence of the characteristic peak $(\text{Sn}-\text{OH})^+$ at $m/z = 137$.

From the above results and observations, the mechanism in Scheme 1 can be put forward. By oxidation of the primary radical R^\cdot by oxygen, a peroxy radical RO_2^\cdot is formed. Peroxy radicals undergo a head-to-head termination reaction to form unstable intermediate tetroxides ROOOOR .³³ The decomposition of tetroxides to give molecular oxygen and two alkoxy radicals is a well-known reaction. The β -scission of the alkoxy radicals is the typical decomposition pathway reported in the literature.³⁴

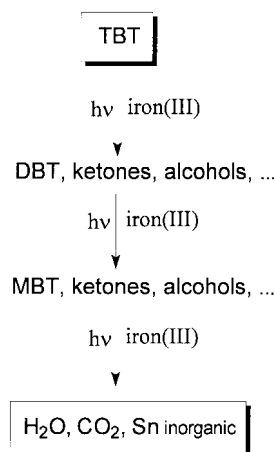
- The scission of the Sn-C bond gives rise to the cation radical $(\text{Bu})_2\text{-Sn}^{\cdot+}$ and by reaction with iron(III) leads to the formation of dibutyltin.
- The scission of the C-H bond leads directly to the formation of the ketone derivative.

A similar mechanism may be described for DBT and MBT.

In aerated solution R^\cdot mainly reacts with oxygen. The formation of alcohol according to Eqn [9] is only of importance in the absence of oxygen (the formation of alcohols is increased by a factor of five under these conditions).



For long irradiation times, we observed the total disappearance of TBT and the photoproducts. Tributyltin was successively debutylated to di- and monobutyltin, with the final formation of inorganic tin. A complete mineralization of TBT was thus obtained (Scheme 2). It is worth noting that this



Scheme 2 Total debutylation of TBT.

chain of reactions leads to a step-by-step reduction of the toxicity down to totally innocuous inorganic tin.

CONCLUSION

The present work illustrates the efficiency of photochemical TBT degradation when the process is photoinduced by iron(III). The photolysis of $\text{Fe}(\text{OH})^{2+}$ produces $\cdot\text{OH}$ radicals. The degradation of TBT under these conditions is only due to attack by these $\cdot\text{OH}$ radicals. The primary step of the decomposition of TBT involves hydrogen abstraction from the carbon atoms in the positions α and β to the tin atom, giving rise to different organotin derivatives. The main route of degradation is a stepwise debutylation of TBT. For long irradiation times, we observed the total mineralization of TBT.

Acknowledgements: This work was realized with the support of CNRS, in the GDR MEMOTOX framework of the 'Environnement Vie et Société' programme.

REFERENCES

1. S. J. Blunden and C. J. Evans, Organotin compounds. In: *Handbook of Environmental Chemistry*, Vol. 3, Part E, Anthropogenic Compounds, Springer Verlag, New York, 1990.
2. WHO *Tributyltin Compounds*, Environmental Health Criteria 116, World Health Organization, Geneva, 1990.
3. C. Alzieu, M. Heral, Y. Thibaud, M. J. Dardignac and M. Fauillet, *Rev. Trav. Inst. Pech. Marit.* **45**, 100 (1982).
4. A. R. Beaumont and M. D. Budd, *Mar. Pollut. Bull.* **15**(11), 402 (1984).
5. L. W. Hall, S. J. Bushong, S. W. Hall and E. W. Johnson, *Environ. Toxicol. Chem.* **7**, 41 (1988).
6. K. Fent, *Mar. Environ. Res.* **28**, 477 (1989).
7. K. Fent, J. Hunn, D. Renggli and H. Siegrist, *Mar. Environ. Res.* **32**, 223 (1991).
8. N. Watanabe, S. Sakai and H. Takatsuki, *Chemosphere* **31**(3), 2809 (1995).
9. E. A. Clark, R. M. Sterrit and J. N. Lester, *Environ. Sci. Technol.* **22**(6), 600 (1988).
10. P. F. Seligman, J. G. Grovhoug, A. O. Valkirs, P. M. Stang, R. Fransham, M. O. Staallard, B. Davidson and R. F. Lee, *Appl. Organometal. Chem.* **3**, 31 (1989).
11. N. Watanabe, S. Sakai and H. Takatsuki, *Water Sci. Tech.* **25**(11), 117 (1992).
12. P. H. Dowson, J. M. Bubb, T. P. Williams and J. N. Lester, *Water Sci. Tech.* **28**(8–9), 1133 (1993).
13. R. J. Maguire, J. H. Carey and E. J. Hale, *J. Agric. Food Chem.* **31**, 1060 (1983).
14. R. J. Maguire and R. J. Tkacz, *J. Agric. Food Chem.* **33**, 947 (1985).
15. K. Duhamel, G. Blanchard, G. Dorange and G. Martin, *Appl. Organometal. Chem.* **1**, 133 (1987).
16. J. A. Navio, F. J. Marchena and C. J. Cerrillos, *Photochem. Photobiol. A: Chem.* **71**, 97 (1993).
17. J. A. Navio, C. Cerrillos, F. J. Marchena, F. Pablos and M. A. Pradera, *Langmuir* **12**, 2007 (1996).
18. P. Mazellier, G. Mailhot and M. Bolte, *New J. Chem.* **21**, 389 (1996).
19. N. Brand, G. Mailhot and M. Bolte, *Chemosphere* **34**(12), 2637 (1997).
20. P. Mazellier, J. Jirkovsky and M. Bolte, *Pestic. Sci.* **49**, 259 (1997).
21. G. Mailhot and M. Bolte, unpublished results.
22. J. G. Calvert and J. M. Pitts, *Photochemistry*, John Wiley, New York, 1966 p. 783.
23. C. Carlier-Pinasseau, G. Lespes and M. Astruc, *Appl. Organometal. Chem.* **10**, 505 (1996).
24. W. H. Kuenzi, PhD Dissertation ETH no. 7016, Eidgenossischen Technischen Hochschule, Zurich, Switzerland, 1982.
25. B. C. Faust and J. Hoigné, *Atmos. Environ.* **24A**(1), 79 (1990).
26. R. J. Knight and R. N. Sylva, *J. Inorg. Nucl. Chem.* **37**, 779 (1975).
27. H. -J. Benkelberg and P. Warneck, *J. Phys. Chem.* **99**, 5214 (1995).
28. C. H. Langford and J. H. Carey, *Can. J. Chem.* **53**, 2430 (1975).
29. ECETO *The Phototransformation of Chemicals in Water. Result of Ring Test*, Technical report no. 12, 1984.
30. R. Franck and W. Klöpffer, *Chemosphere* **17**(5), 985 (1988).
31. M. Pereyre, B. Bellegarde, J. Mendelson and J. Valade, *J. Organometal. Chem.* **11**, 97 (1968).
32. I. F. Lutsenko, Y. I. Baukov and I. Y. Belavin, *J. Organometal. Chem.* **24**, 359 (1970).
33. J. E. Bennett and J. A. Howard, *J. Am. Chem. Soc.* **95**(12), 4008 (1973).
34. C. von Sonntag and H. P. Schuchman, *Angew. Chem., Int. Ed. Engl.* **30**, 1229 (1991).